

Analysis of a Concentrated Winding Induction Machine for Adjustable Speed Drive Applications

Part 2 (Motor Design and Performance)

Hamid A. Toliyat Thomas A. Lipo
Student Member, IEEE Fellow, IEEE
University of Wisconsin-Madison
1415 Johnson Drive
Madison, WI 53706

J. Coleman White
Life Fellow, IEEE
Electric Power Research Inst.
3412 Hillview Ave.
Palo Alto CA 94303

Keywords: Concentrated Windings, Adjustable Speed Drive, Induction Machines, Simulation

Abstract - The performance of multiphase concentrated winding induction machines specifically designed for operation with static power converters is described. The winding distributions are intentionally rectangular to better accommodate the rectangular wave forms of solid state inverters. Fourier analysis is used for investigation of the effects of different air-gap field spatial distributions and time harmonics in the supply. The approach to analysis of such machines, derived in Part I, is implemented by means of a digital computer simulation. Computed results indicate that when operating in conjunction with a converter supply, a specially wound five phase machine is theoretically capable of a 10% improvement in torque per rms ampere assuming the same peak air-gap flux density level in the air-gap of the machine as in a conventionally designed induction motor of the same rating.

1. Introduction

In Part I, the differential equations of an m phase induction machine with concentrated full pitch windings were derived. The rotor of the machine was analyzed by considering that the current in each bar was an independent variable. Hence, the effects of non-sinusoidal air gap MMF produced by both the stator and the rotor currents have been incorporated into the model. In Part II these equations are applied to the analysis of a machine fed from an m phase current source inverter and the possibility of improved torque per rms ampere for such machines investigated.

2. Harmonic Analysis of Induction Machines with Nonsinusoidal Space and Time Distribution

While a detailed simulation of the machine differential equations is required to properly determine motor waveforms under load, considerable insight into motor performance can be gained by simply investigating the characteristics of the impressed air gap MMF waveform. The concept of winding functions combined with Fourier analysis provides a useful tool for this purpose in order to evaluate the effects of different air-gap field spatial distributions and time harmonics in the supply. In this section it will be assumed:

- the machine is considered to be operating in the steady state under a zero load condition.
- saturation effects are neglected to allow superposition of magnetic fields.
- skin effects in the stator conductors at the harmonic frequencies are neglected.

Consider a stator of an induction machine with the elementary two pole, three phase concentrated windings which are 120 degrees apart in space as shown in Fig. 2(a) of Part I. The winding function for each phase is given in Fig. 3(a) of Part I. The Fourier series of each winding is as follows:

$$N(\phi) = \sum_{n=1}^{\infty} \left(\frac{4}{n\pi} \right) \frac{N}{2} \sin \frac{n\pi}{2} \cos n(\phi + \alpha) \quad (1)$$

91 WM 0052-1 EC A paper recommended and approved by the IEEE Electric Machinery Committee of the IEEE Power Engineering Society for presentation at the IEEE/PES 1991 Winter Meeting, New York, New York, February 3-7, 1991. Manuscript submitted August 27, 1990; made available for printing December 18, 1990.

where α is the spatial angle between the phases. Since the winding functions are symmetric, even space harmonics do not exist. As a typical example of a prescribed type of excitation let us assume that this machine is operated in conjunction with a current source inverter (CSI). In this case each coil carries a quasi-rectangular current as given in Fig. 1. The Fourier series of the current waveforms are given by

$$i(\theta) = \sum_{m=1}^{\infty} \left(\frac{4}{m\pi} \right) I_m \cos \frac{m\pi}{6} \sin m(\theta + \delta) \quad (2)$$

where

$$\theta = \omega t$$

and δ is an arbitrary phase angle. Since the current waveforms are symmetric, it is clear that even harmonics again can not exist.

The spatial MMF pattern at any instant resulting from the coil currents is decided by the instantaneous currents in all the coils. The rotational movement of the pattern with time is decided by the time variation of these currents; i.e. the current waveforms. Let F be the total MMF's produced by coils a, b, c. Then

$$F = N_a i_a + N_b i_b + N_c i_c = \sum_{n=1}^{\infty} \sum_{m=1}^{\infty} \left(\frac{1}{n\pi} \right) \left(\frac{4}{\pi} \right) \frac{N I_m}{2} \sin \frac{n\pi}{2} \cos \frac{m\pi}{6} \left(\sin(m\theta - n\phi) \left(\cos \frac{(m-n)2\pi}{3} + \frac{1}{3} \right) + \sin(m\theta + n\phi) \left(\cos \frac{(m+n)2\pi}{3} + \frac{1}{2} \right) \right) \quad (3)$$

The two major terms in the expression above represent a pair of air-gap fields, the first field rotating forward and the other backward.

3. Harmonic Analysis of 3, 6, and 9 phase Induction Machines (Type I)

Using the concepts developed in the previous section it is possible to determine the air-gap field for cases of different numbers of phases [1]. In this section three different numbers of phases are examined: 3, 6, and 9 phase machines. In particular, Table 1 shows the MMF's present in the air gap for a 3 phase case. In Table 1 a plus sign indicates those MMF's which are rotating forward while a negative sign represents those rotating backward. It is interesting to note that those MMF's which are produced by the same order of space and time harmonics rotate forward at synchronous speed. All others are rotating at speeds equal to n/m times synchronous speed, some in the forward direction and some backward. It is clear that all multiples of third harmonic are eliminated in the case of a three phase connection without a neutral return. Note that the effects of the higher harmonics are essentially to reduce the average torque. For example, the fifth time harmonic combines with the fifth space harmonic to produce a positive torque of 0.042NI. However, the fifth harmonic in time flowing in the first time harmonic has an amplitude of 0.122NI which

		SPACE HARMONICS							
		1	3	5	7	9	11	13	15
TIME HARMONICS	1	+1.053		-.211	+.150		-.096	+.081	
	3								
	5	-.211		+.042	-.030		+.019	-.016	
	7	+.150		-.030	+.021		-.014	+.012	
	9								
	11	-.096		+.019	-.014		+.009	-.007	
13	+.081		-.016	+.012		-.007	+.006		
15									

Table 1 Relationships between field space harmonics and current time harmonics for a 3-phase winding.

results in a negative torque exceeding the positive contribution. In addition the fundamental time harmonic flows through the fifth space harmonic causing an additional negative torque produced with an amplitude of 0.211NI.

It is possible to generalize this concept to higher order phase numbers. Figures 1 shows an idealized diagram of a six phase concentrated winding induction machine. A six phase machine can be easily constructed by splitting the 60 degree phase belt into two portions each spanning 30 degrees. Thus the machine consists of two groups of symmetrical three phase windings, a1, b1, c1, and a2, b2, c2, with CSI-1 feeding the first group and CSI-2 feeding the second group. Since there is a 30 electrical degree phase shift between the phase groups, the CSI-2 line current is delayed by 30 electrical degrees with respect to that of the corresponding phase in CSI-1. The commutation process in CSI-1 and CSI-2 is similar to that of the conventional source. Table 2 shows the MMF present for 6 phase winding. Comparing with Table 1 it can be seen that the array of unwanted harmonics is shifted to higher orders where their effect in terms of losses and low speed torque pulsations diminish roughly in inverse proportion to their order. In particular, note that the fifth and seventh harmonics now contribute a net positive torque (0.042NI) while interacting only with each other (and not the first harmonic).

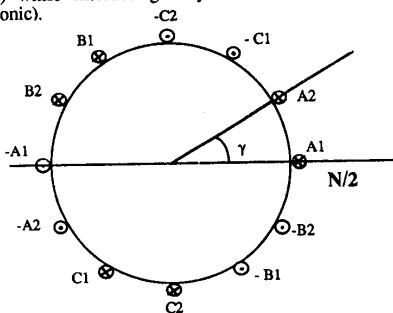


Figure 1 Winding configuration of a 6-phase concentrated winding.

		SPACE HARMONICS													
		1	3	5	7	9	11	13	15						
TIME HARMONICS	1	+1.053													
	3														
	5			+0.042	-0.030										
	7				-0.030	+0.021									
	9														
	11							+0.009	-0.007						
	13									-0.007	+0.006				
	15														

* MULTIPLY BY NI

Table 2 Relationship between field space harmonics and current time harmonics for a 6-phase winding.

It is possible to again generalize the same idea to a 9 phase winding. In this case the 60 degree phase belt is split into three portions each spanning 20 electrical degrees. The machine consists of three groups of symmetrical 3 phase windings namely a1, b1, c1, and a2, b2, c2, and a3, b3, c3. Since there is a 20 electrical degree phase shift between each group, the three 3-phase CSI are shifted with respect to each other by 20 degrees. The results of a harmonic analysis for this case is depicted in Table 3. Again, as expected, the off-diagonal fields have been moved to higher frequencies with respect to the 6 phase winding. In this case both the fifth and seventh harmonics produce net torque without any detrimental interaction (such as pulsating torque). It is obvious that in all three cases the multiple of the third harmonic should be missing.

		SPACE HARMONICS												
		1	3	5	7	9	11	13	15					
TIME HARMONICS	1	+1.053												
	3													
	5			+0.042					-0.016					
	7				+0.021			-0.014						
	9													
	11									+0.009				
	13													+0.006
	15													

* MULTIPLY BY NI

Table 3 Relationship between field space harmonics and current time harmonics for a 9-phase winding.

4. Harmonic Analysis of 5, 7, and 9 phase Induction Machines (Type II)

In the previous section the analysis for 3, 6, and 9 phase machines was considered in which the input current source consisted of 120 electrical degrees pulses. Hence, the machine was assumed to be fed by groups of three phase current source inverters in which the sum of the current in each of the three phase groups summed to zero. In this section, a 5 phase machine is examined, which is fed from an inverter supply wherein the electrical pulses can be adjusted to values greater than 120 degrees. In this case the five currents are assumed to sum to zero so that the machine is again star connected. Although a conventional current source inverter can not be used as the supply, such a waveform can be realized by a five phase PWM inverter as shown in Figure 2. The five phases are placed such that the spatial angle between each two phases is $2\gamma = 72$ degrees, see Fig. 3-(a). The input current is given in Fig. 3-(b) which consists of 144 degrees pulses. Table 4 shows the MMF present for the 5 phase case. It is obvious that in this case we have the third harmonic, which is produced by third time and space harmonics rotating forward, and the fifth harmonic is eliminated. Pulsating torques below the seventh harmonic are eliminated.

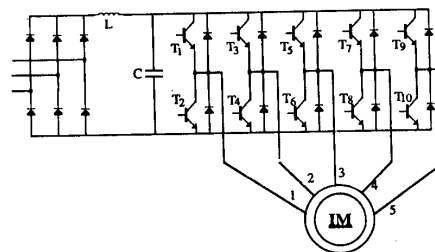


Figure 2 Five phase pulse-width-modulated inverter.

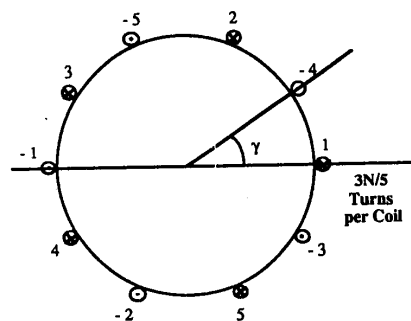


Figure 3-(a) Winding configuration of a 5-phase concentrated winding machine.

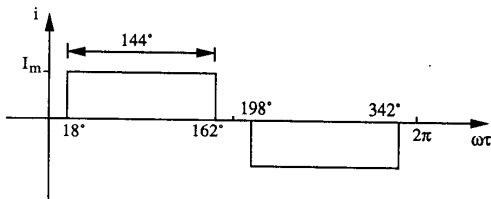


Figure 3-(b) Current waveform for a 5-phase induction machine.

		SPACE HARMONICS																	
		1	3	5	7	9	11	13	15										
TIME HARMONICS	1	+1.056																	
	3		+0.072																
	5																		
	7																		
	9																		
	11																		
	13																		
	15																		

* MULTIPLY BY NI

Table 4 Relationship between field space harmonics and current time harmonics for a 5-phase winding.

It is possible to generalize this idea to 7 and 9 phase cases. In the 7 phase case the spatial angle between two phases is $2\gamma=51.43$ degrees. The input currents are pulses of 154.3 instead of 120 degrees. Table 5 summarizes the field harmonics up to the 15th space and time harmonics. Again the third harmonic exists, whereas multiples of the 7th harmonic are removed. The first, third and fifth harmonics all act to produce average torque. Pulsating torques below the thirteenth harmonic are eliminated.

		SPACE HARMONICS																	
		1	3	5	7	9	11	13	15										
TIME HARMONICS	1	+1.045																	
	3		+0.093																
	5																		
	7																		
	9																		
	11																		
	13																		
	15																		

* MULTIPLY BY NI

Table 5 Relationship between field space harmonics and current time harmonics for a 7-phase winding.

Finally, the Type II 9 phase machine is one with a spatial angle between adjacent phases of $2\gamma=40$ degrees. The input current is now comprised of 160 degree pulses. Table 6 illustrates the result of harmonic analysis of the field. It is interesting to note that only the multiples of the 9th harmonic are missing and that the first, third, fifth and seventh time harmonics all rotate synchronously through their respective space harmonic windings to produce average torque.

It is clear that the useful operating region of an induction machine is that region where the rotor operates near synchronous speed. Hence, only those fields rotating at synchronous speed will produce useful torque. Fields rotating at much higher speeds will produce very little torque, whereas those fields rotating at speeds less than synchronous, or are rotating backwards will reduce the total torque. When the phase number is increased, the low speed torque pulsation frequency increases with the phase number and its amplitude decreases rapidly.

		SPACE HARMONICS																		
		1	3	5	7	9	11	13	15											
TIME HARMONICS	1	+1.037																		
	3		+0.101																	
	5																			
	7																			
	9																			
	11																			
	13																			
	15																			

* MULTIPLY BY NI

Table 6 Relationship between field space harmonics and current time harmonics for a 9-phase winding.

Phase numbers of the order 3, 6, or 9 with currents in 2, 4 or 6 phases at any instant are all equivalent in terms of their fundamental flux producing capability. That is, for the same copper losses and the same copper weight the peak fundamental air gap MMF is 1.053NI for all three cases. However, in type II excitation with phase numbers of the order 5, 7, 9 etc., 4, 6, 8 etc. phases carry current at any instant. In this case the fundamental MMF produced by the 5 phase winding exceeds the usual three phase winding by a small amount (1.056NI). In addition, useful MMF is produced by the third harmonic MMF which rotates synchronously with the fundamental component (0.072NI). When a 7 phase winding is used, the fundamental MMF component actually decreases to 1.045NI while the third harmonic component increases to 0.093NI.

Table 7 summarizes the results of the harmonic analysis. Listed for each winding configuration are only those terms on the "diagonal" which produce torque without introducing a detrimental backward field component. For example, for the 5 phase winding of Table 4, the first and third harmonic components produce net positive torque but the pulsating torque arising from the first harmonic MMF rotating through the third winding harmonic, and vice versa, are identically zero. However, the seventh harmonic component, while producing an average torque of 0.013 also produces a backward field of amplitude 0.031 (produced by the third time harmonic rotating in the seventh space harmonic and vice versa) so that its contribution cannot be considered as useful. Since torque is essentially proportional to the square of the MMF, the sum of the squares of the "useful" harmonics is shown for comparison. It is interesting to note that with this basis for comparison the five phase machine has the optimum torque per rms ampere. While the improvement is small, it will be shown in the next chapter that the altered shape of the air gap MMF permits a substantial increase in output torque of the machine.

Phase Number	Amplitude of Useful MMF Harmonics				Performance Index
3 phase	1.053	0	0	0	1.1088
6 phase	1.053	0	0	0	1.1088
9 (120°)	1.053	0	0.042	0.021	1.1110
5 phase	1.056	0.072	0	0	1.1203
7 phase	1.045	0.093	0.019	0	1.1010
9 (160°)	1.037	0.101	0.027	0.007	1.0857

Table 7 Summary of MMF harmonics for six types of current fed induction machines.

$$\text{Perf. Index} = \sum_{n=1,3,5,7}^7 \left(\frac{\text{MMF}_n}{NI} \right)^2$$

5. Digital Computer Simulation Results

The Fourier analysis of the previous section has demonstrated the rather marginal benefits of rectangular rather than sinusoidal MMF for the purpose of increasing the torque per rms ampere of an induction machine. However, the MMF that was considered involved only the impressed stator MMF, and a more detailed analysis must be undertaken to establish its true potential. The new computer simulation model developed in the

previous chapter, however, affords the computational tool needed to examine the air gap fields when the machine is under load, i.e. when the MMF due to the rotor current is accounted for.

The concept of a uniformly rotating rectangular field can be better visualized by first considering a stator with q separate full-pitch coils. When each coil is excited in sequence an air-gap field is produced which steps around the air-gap in intervals of π/q radians. When $q=3$, as in a 3 phase machine, the discontinuities caused by the large 60 degree steps between coils generate undesirable losses and spurious torques. As q increases, however, the steps become smaller and the disturbances caused by stepping become less and less significant. In the limit as q becomes large, the field tends towards a smoothly rotating rectangular field. In a squirrel cage induction motor this field induces a rectangular voltage in the rotor bars. If the rotor leakage inductance is ignored, the result is a rectangular rotor current which is aligned with the flux. This results in a rectangular net air-gap field with maximum utilization of the air-gap iron.

The harmonic analysis of section two reveals that the improvement which is gained by increasing the number of phases in the first study (3, 6, 9 phase machine with 120 degree pulses) is essentially obtained by shifting the array of unwanted harmonics to higher frequencies. Such a motor design would result in lower torque pulsations and less rotor harmonic losses. Consequently, we expect that for the same rms input current the output power will increase. The same argument seems valid in the second study (5, 7, 9 phase). The main difference in this case is that the third harmonic exists, producing useful torque and, we will soon learn, reducing the peak air gap flux density within the machine. In this chapter we will use the computer model which was developed in chapter three to simulate the induction machine operating from a current fed converter.

It is again worth mentioning that the well established d-q equations are not used for this simulation study because these equations were developed by assuming that the air-gap field in the machine is sinusoidal. In the case under study, however, we seek a rectangular air-gap field. A digital computer simulation using ACSL (Advanced Continuous Simulation Language) has been developed which, with some modification, handles any number of stator phases and rotor bars.

6. Simulation Results of Machines of the First Type (3, 6, and 9 phase with 120-degree pulses)

In this portion of the investigation an eight pole induction motor with 3, 6 or 9 phases was simulated. The machine studied was assumed to have 24 stator slots in case of 3 phase, 48 in case of 6 phase, and 72 stator slots in the 9 phase case. In each case a machine with 40 rotor bars has been simulated. It is assumed that the motor shaft is rotating at constant speed and in order to compare machines with different phase number, it is assumed that the total rms current and the total air-gap flux in each machine is held constant. Hence, if the resistance for each winding is assumed reasonably constant, the copper losses associated with the stator remain essentially constant. Since the total flux is the same, the stator core cross section as well as the stator copper cross sectional area remain the same for all machines so that the machines physically have the same frame size.

Figures 4(a) to 4(c) depict the rotor flux linkages for the three types of stator construction. This rotor flux corresponds to the flux linkage of a single rotor tooth. Since the bars are, of course, concentrated, this plot is also effectively the equivalent to the air gap flux density. It can be recalled from the harmonic analysis of the previous chapter that great differences in the wave shapes are not expected. It can be noted that the amplitude of the flux linkage (or air gap flux density) is almost the same, having a nearly sinusoidal shape even with an increasing number of phases.

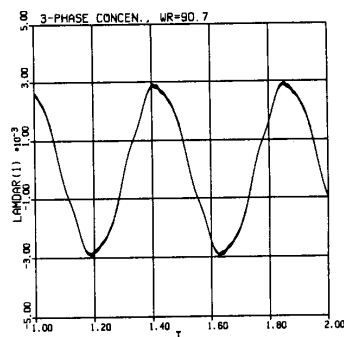


Figure 4-(a) Rotor flux linkage waveform of 3 phase machine for Type I operating at 60 Hz. Rotor speed = 866 RPM.

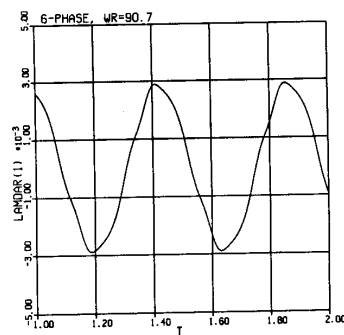


Figure 4-(b) Rotor flux linkage waveform of 6 phase machine for Type I operating at 60 Hz. Rotor speed = 866 RPM.

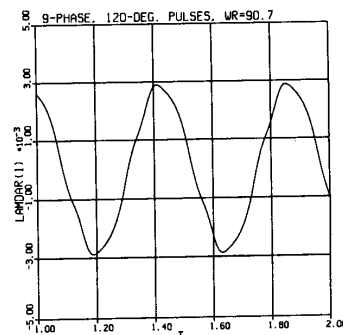


Figure 4-(c) Rotor flux linkage waveform of 9 phase machine for Type I operating at 60 Hz. Rotor speed = 866 RPM.

Figures 5(a) to 5(c) portray the instantaneous electromagnetic torque. It should be noted that the high frequency pulsations observed on the torque waveform result from the manner in which the machine was modeled. In practice, the winding functions do not have the discontinuous derivatives of the functions of Figure 4 of Part I. Since the winding functions have been modeled with "sharp edges" (discontinuous derivatives), the mutual inductances between stator and rotor have "sharp corners" (discontinuous second derivatives). Hence, the torque as defined by Eq. (27) of Part I shows a higher harmonic content of torque pulsations than the actual case. Note, however, that the torque pulsation reduces for the higher number of phases as expected.

To have a better estimate of the value of electromagnetic torque, a first order filter has been used to filter out the unnecessary torque pulsations and provide a more realistic impression of the average torque. The final results are depicted in Figs. 6(a) to 6(c). With an increasing number of phases the output torque increases very slightly, which is due to the reduction of the rotor copper losses. We have already mentioned in chapter two that increasing number of phases results in shifting the array of unwanted harmonics to higher frequencies with smaller amplitude.

Figures 7(a) to (c) illustrate the current in a single rotor bar for the three types. Note the reduction in the ripple current superimposed on the main (slip frequency) current, which accounts for the slight improvement in efficiency as the phase number increases. Shown in Figures 8(a), to (c) are the terminal voltages. Note that since the stator leakage inductance decreases with increasing phase number, the magnitudes of terminal voltage spikes reduce. This feature is especially important for operation with a solid state converter supply since the voltage rating of the converter switches is essentially determined by the motor leakage inductance. Hence, while the number of switches increases with an increasing number of phases, the volt-ampere rating of the individual switches decreases, keeping the total volt-ampere rating of the total number of switches roughly the same.

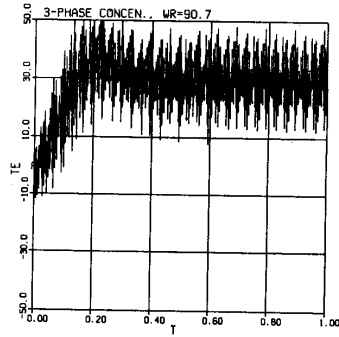


Figure 5(a) Instantaneous electromagnetic torque waveform of 3 phase machine operating at 60 Hz. Rotor speed = 866 RPM.

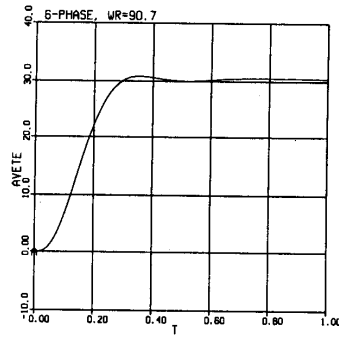


Figure 6(b) Average electromagnetic torque waveform of 6 phase machine operating at 60 Hz. Rotor speed = 866 RPM.

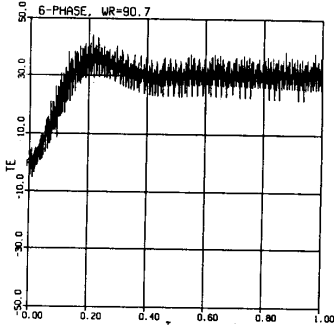


Figure 5(b) Instantaneous electromagnetic torque waveform of 6 phase machine operating at 60 Hz. Rotor speed = 866 RPM.

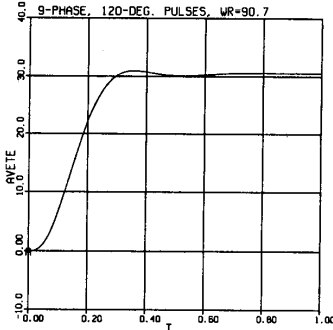


Figure 6(c) Average electromagnetic torque waveform of 9 phase machine operating at 60 Hz. Rotor speed = 866 RPM.

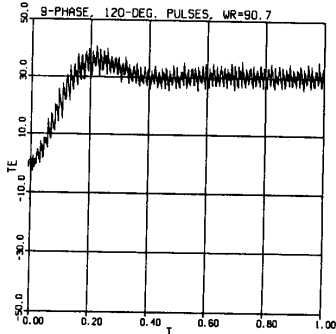


Figure 5(c) Instantaneous electromagnetic torque waveform of 9 phase machine operating at 60 Hz. Rotor speed = 866 RPM.

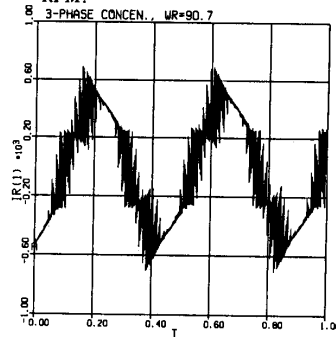


Figure 7(a) Rotor bar current waveform of 3 phase machine operating at 60 Hz. Rotor speed = 866 RPM.

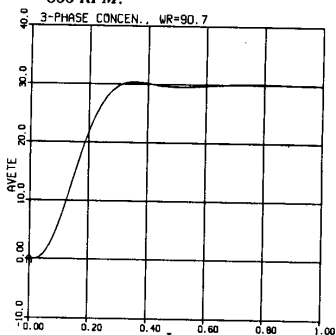


Figure 6(a) Average electromagnetic torque waveform of 3 phase machine operating at 60 Hz. Rotor speed = 866 RPM.

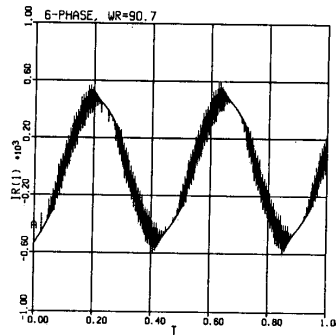


Figure 7(b) Rotor bar current waveform of 6 phase machine operating at 60 Hz. Rotor speed = 866 RPM.

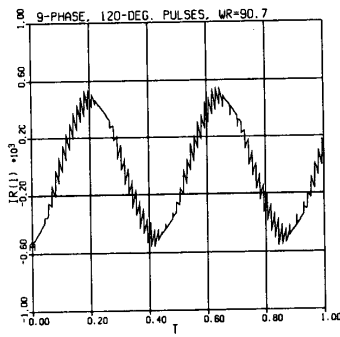


Figure 7(c) Rotor bar current waveform of 9 phase machine operating at 60 Hz. Rotor speed = 866 RPM.

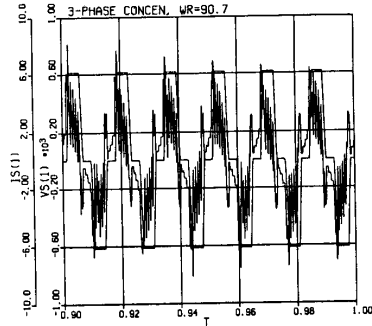


Figure 8(a) Terminal voltage waveform of 3 phase machine operating at 60 Hz. Rotor speed = 866 RPM.

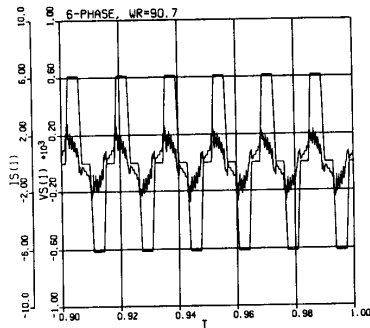


Figure 8(b) Terminal voltage waveform of 6 phase machine operating at 60 Hz. Rotor speed = 866 RPM.

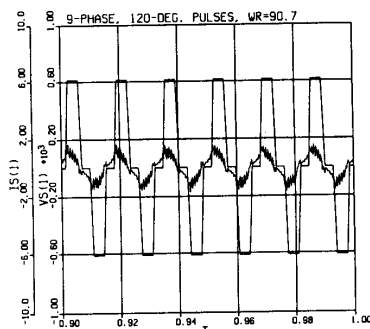


Figure 8(c) Terminal voltage waveform of 9 phase machine operating at 60 Hz. Rotor speed = 866 RPM.

7. Simulation Results of Machines of the Second Type (5, 7, and 9 phase)

In this case the 5, 7, and 9 phase induction motors have been modeled with the same physical dimensions as for the Type I machines. The current source converter switches are assumed to conduct for 144° in the 5 phase case, 154.3° for the 7 phase, and 160 electrical degrees for the 9 phase case. The eight pole machine is assumed to have 40 stator slots in the case of 5 phase, 56 in the case of 7 phase, and 72 stator slots for the 9 phase case. Again, similar to the previous case, the rms value of the total stator current was maintained constant.

Figures 9(a), to (c) provide traces of the electromagnetic torque. To have a better estimate of the value of the electromagnetic torque, a first order filter has again been used to filter out the unnecessary torque pulsations and provide us with the average torque. The final results are depicted in Figures 10(a), to 10(c). With an increasing number of phases the output torque is increasing, which is due to a reduction in the rotor copper losses. We have already mentioned in chapter two that increasing the number of phases results in shifting the array of unwanted harmonics to higher frequencies with smaller amplitude. Figures 11(a) to (c) show the current in one of the rotor bars. Shown in Figs. 12(a), to (c) are the terminal voltages. Again it can be noted that due to the reduction of the stator leakage inductance, the magnitude of terminal voltages reduces with increasing the number of phases.

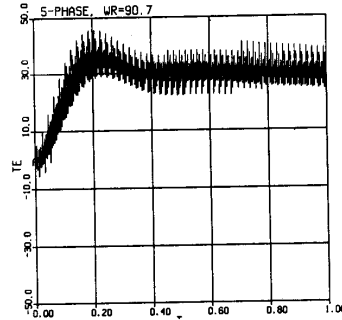


Figure 9(a) Instantaneous electromagnetic torque waveform of 5 phase machine operating at 60 Hz. Rotor speed = 866 RPM. Type II.

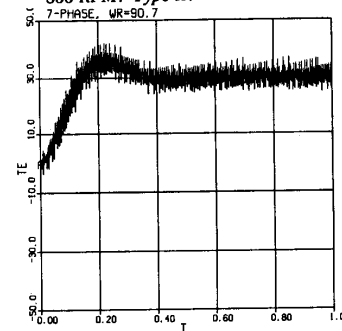


Figure 9(b) Instantaneous electromagnetic torque waveform of 7 phase machine at 60 Hz and 866 RPM. Type II.

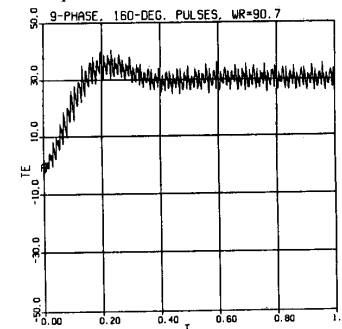


Figure 9(c) Instantaneous electromagnetic torque waveform of 9 phase machine at 60 Hz and 866 RPM. Type II.

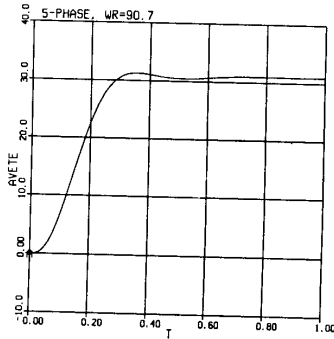


Figure 10(a) Average electromagnetic torque waveform of 5 phase machine at 60 Hz and 866 RPM. Type II.

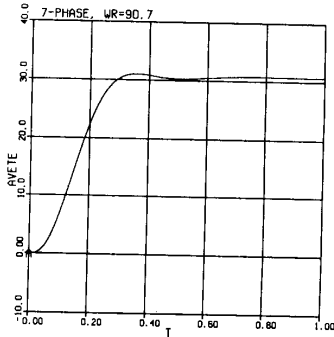


Figure 10(b) Average electromagnetic torque waveform of 7 phase machine at 60 Hz and 866 RPM. Type II.

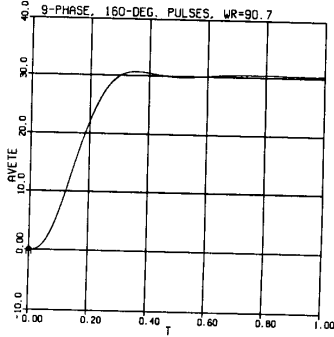


Figure 10(c) Average electromagnetic torque waveform of 9 phase machine at 60 Hz and 866 RPM. Type II.

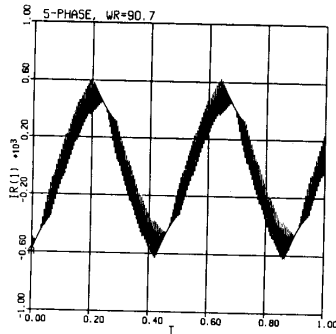


Figure 11(a) Rotor bar current waveform of 5 phase machine at 60 Hz and 866 RPM. Type II

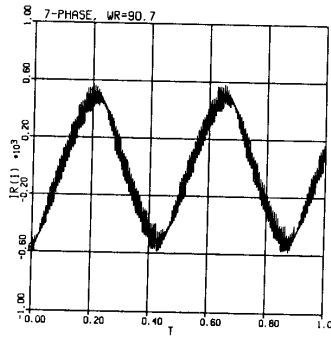


Figure 11(b) Rotor bar current waveform of 7 phase machine at 60 Hz and 866 RPM. Type II.

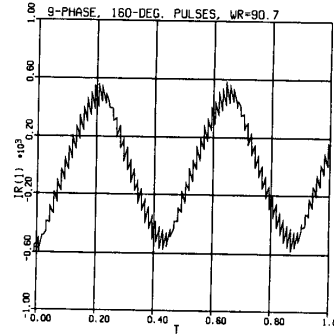


Figure 11(c) Rotor bar current waveform of 9 phase machine at 60 Hz and 866 RPM. Type II.

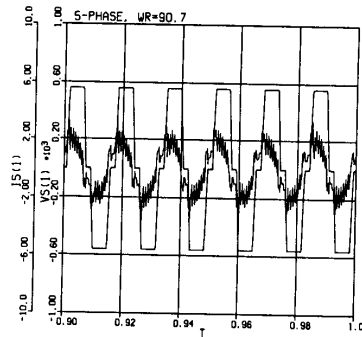


Figure 12(a) Terminal voltage waveform of 5 phase machine at 60 Hz and 866 RPM. Type II.

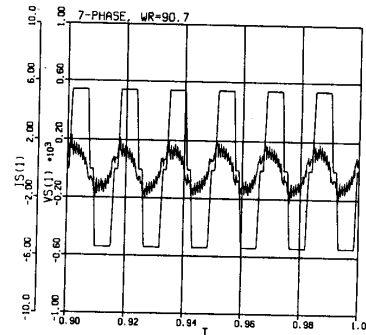


Figure 12(b) Terminal voltage waveform of 7 phase machine at 60 Hz and 866 RPM. Type II.

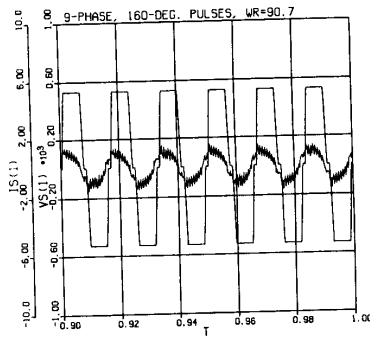


Figure 12-(c) Terminal voltage waveform of 9 phase machine at 60 Hz and 866 RPM. Type II.

Figures 13(a), to (c) illustrate the rotor flux linkages of a single bar for this case. Again since the bars are concentrated, this waveform is effectively identical to the flux density waveform in the air gap. It can be noted that from the harmonic analysis of Part I that the existence of a third harmonic field can be expected. It is particularly important to note that the amplitude of the flux linkages (air gap flux density) is now less than for Type I and decreases with an increasing number of phases. It is also important to note that the waveform begins to approach a rectangular wave shape. In general, the peak air gap flux density is set by the iron saturation flux paths. Since the peak flux density has been reduced it is therefore possible to decrease the rotor slip (increase the speed) and thereby increase the flux and consequently the torque while keeping the rms current constant. By trial and error the correct values of slip were found in each case. Figures 14(a), to (c) depict the corresponding electromagnetic torque. Note that a 10% increase in torque appears to be possible for the 5 phase machine while a slightly smaller increase in torque in the 9 phase case can be obtained.

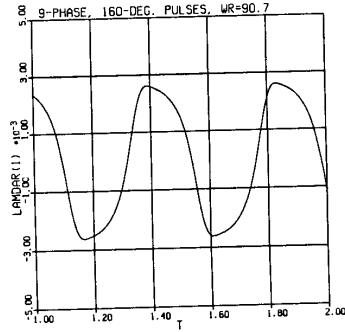


Figure 13-(c) Rotor flux linkages waveform of 9 phase machine at 60 Hz and 866 RPM. Type II.

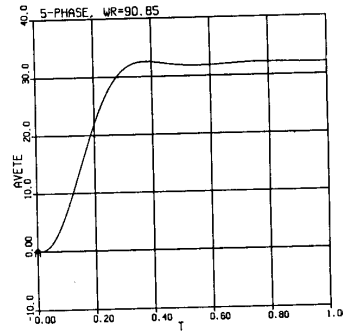


Figure 14-(a) Average electromagnetic torque waveform of 5 phase machine at 60 Hz, 867.6 RPM and same flux level as Type I.

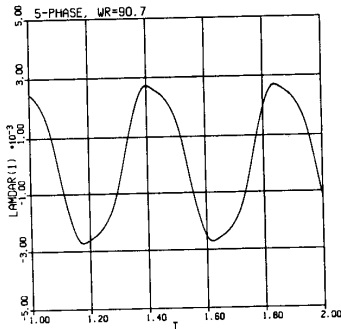


Figure 13-(a) Rotor flux linkages waveform of 5 phase machine at 60 Hz and 866 RPM. Type II.

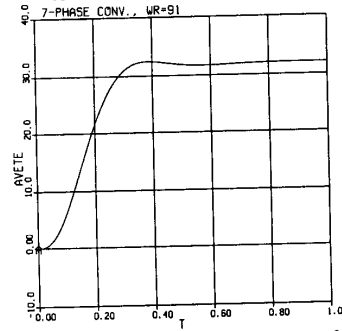


Figure 14-(b) Average electromagnetic torque waveform of 7 phase machine at 60 Hz, 869 RPM and same flux level as in Type I.

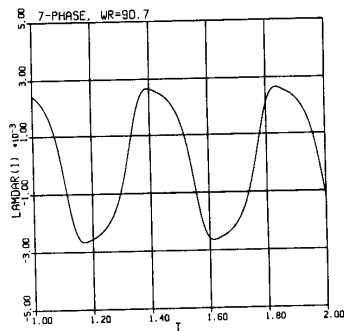


Figure 13-(b) Rotor flux linkages waveform of 7 phase machine at 60 Hz and 866 RPM. Type II.

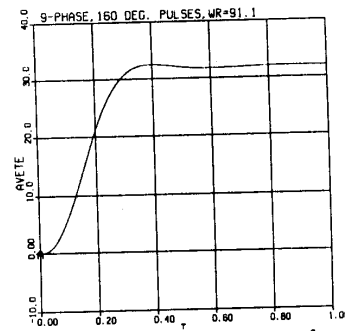


Figure 14-(c) Average electromagnetic torque waveform of 9 phase machine at 60 Hz, 870 RPM and same flux level as in Type I.

8. Conclusion

This paper presents a summary of the key analytical and simulation results obtained during an investigation of multiphase concentrated winding induction motors excited by voltage source or current source inverters. The concentrated winding machine is essentially one in which all phases have a pitch, skew and distribution factor equal to unity. Two generic types of excitation have been identified. In the first type, the machine is excited with multiple sets of conventional auto-sequentially commutated three phase bridges. Hence, such machines only have a phase number equal to a multiple of three, that is 3, 6, 9 etc. In this case, the currents in each semiconductor switch consist of 120° blocks of constant amplitude current. Specifically in Type I, the 6 phase squirrel cage induction motor consists of two three-phase concentrated stator winding sets separated by 30 electrical degrees. The 9 phase induction motor consists of three three-phase stator winding sets separated by 20 electrical degrees with respect to each other. In the second configuration, Type II, the machine is equipped with an odd number of phases wherein $N-1$ of the N phases conduct current. In the five phase motor each semiconductor switch carries a 144° block of constant amplitude current. For the 7 phase motor each switch has a 154.3° constant current waveform per cycle. Finally, the semiconductor switches associated with the 9 phase motor conduct a 160 electrical degree current waveform.

Fourier analysis has been used for investigation of the effects of different air-gap field spatial distributions and time harmonics in the supply. It has been shown that odd harmonic components of the magnetic field can be made to rotate synchronously with the fundamental and, consequently, produce useful torque. In particular, for Type II configurations it is shown that a synchronous rotating third field harmonic exists produced by the third time and third space harmonic. It is shown, however, that the contribution of these harmonic components for practical converter configurations and phase number is only on the order of 1 or 2%.

An analytical model for the multiphase motor system has been presented based on the general theory of coupled magnetic circuits. The method treats each phase and rotor bar as an independent circuit. This model is used to develop a digital computer program which simulates a multi-phase induction motor. Simulation of the motors of Type I having multiple three phase groups of conventional current source inverters, indicates that if the total stator copper I^2R is held constant, then the peak air gap flux density and electromagnetic torque for 3, 6 and 9 phase machines are essentially identical. It is further shown that for the same conditions, the Type II machines having an odd phase number with $N-1$ of the N phases conducting also result in the same electromagnetic torque for the same stator I^2R losses. However, this electromagnetic torque is achieved with a smaller peak air gap flux density than the Type I machines. Hence, the flux density can be raised by decreasing the rotor slip frequency (increasing the speed at fixed frequency) thereby increasing the torque an additional 10% without changing the stator I^2R losses or peak air gap flux density. In effect, the third harmonic of air gap flux density is used to reduce the peak flux density in much the same manner as the use of an intentional third harmonic component in cycloconverter and PWM inverter drives [2].

The key advantages of Type II multi-phase induction motor drive systems over conventional three phase systems can be summarized as follows

- In general, it is desired to keep the sum of rms values of the motor currents constant to maintain the same stator I^2R losses. However, since the width of the current pulse in each phase is larger than 120° the amplitude of the pulse can be decreased resulting in reduced converter losses.

- The voltage rating of the components of each inverter is reduced since the leakage inductance decreases as the phase number increases, resulting in lower cost solid state switches.

- Since the number of inverter switching events increases with the phase number, the frequency of the low order pulsating torque amplitude increases while its amplitude decreases so that the torque pulsation problem is much less compared to conventional three phase, current source induction motor drives.

- Since the number of inverter switching events increases the amplitude (frequency) of the induced rotor current decreases (increases) respectively resulting in a reduction of rotor harmonic losses from the level produced in a 3 phase, six-step system.

- The overall system reliability is improved by providing more phases.

- The multi-phase concentrated winding induction motors of Type II have the superiority of being able to supply at least 10 percent more torque compared to induction motors of Type I as well as compared to conventional induction motors.

Potential disadvantages of such motor drives include the following

- The number of semiconductor switches increase with the phase number leading to the potential of higher cost. The problem becomes less significant as the size of the machine increases.

- Since the harmonic content of the air gap flux density has been increased with these new machines, the iron loss in the teeth will increase and must therefore be carefully controlled.

This study has suggested that the multiphase concentrated winding induction machines of Type II are capable of producing higher torque with better iron utilization than the machines of Type I. Specifically, from the point of view of torque production, the 5 phase machine appears to be highly desirable. While the number of active switches increases from 6 to 10, the VA rating of each individual switch decreases. Although a simple two pole 5 phase connection is possible, the number of slots dictated by concentrated windings necessitates the use of only 10 stator slots for a two pole machine. However, this slot number appears to be too small for good thermal integrity and also results in windings having a high leakage reactance, which tends to degrade performance. The characteristics of the concentrated winding machine improve as the number of phases and number of poles increases. If the phase number is selected as 5, the number of slots for a four pole machine becomes 20, six pole 30, and eight pole 40, which is a slot number to obtain reasonably good behavior. Therefore, an eight pole five phase machine has been constructed. The hardware implementation of the relevant PWM inverter shown in Figure 3 has also been developed. The test results will be reported in a subsequent paper.

Acknowledgments

This work was sponsored by the Electric Power Research Institute, Palo Alto, CA, under contract number RP 2624-2.

References

- [1] Gosden, D.F., "An Inverter-Fed Squirrel Cage Induction Motor with Quasi-Rectangular Flux Distribution", Electric Energy Conf., October 6-9, 1987, Adelaide, Australia, pp. 240-245.
- [2] Alesina, A. and Venturini, M., "Intrinsic Amplitude Limits and Optimum Design of 9-Switches Direct PWM AC-AC Converters", 1988 Power Electronics Specialist's Conference, Kyoto Japan, April 11-14, 1988, pp. 1284-1291.



Hamid A. Toliyat was born in Mashhad, Iran, in 1957. He received the B.S. (1982) and M.S. (1986) in electrical engineering from Sharif University of Technology, Tehran, Iran and West Virginia University, Morgantown, W.V. respectively. Between 1982 and 1984 he worked for power companies in Iran. He is presently working toward his Ph.D. at the University of Wisconsin-Madison where he is involved with the converter controlled ac machines. Mr. Toliyat is a member of the IEEE and Sigma Xi.



Thomas A. Lipo (M'64-SM'71-F'87) is a native of Milwaukee Wisconsin. He received his B.E.E. and M.S.E.E. degrees from Marquette University, Milwaukee, WI in 1962 and 1964 and the Ph.D. degree in electrical engineering from the University of Wisconsin in 1968. From 1969 to 1979 he was an Electrical Engineer in the Power Electronics Laboratory of Corporate Research and Development of the General Electric Company, Schenectady NY. He became Professor of Electrical Engineering at Purdue University in 1979 and in 1981 he joined the University of Wisconsin in the same capacity.

Dr. Lipo has maintained a deep research interest in power electronics and ac drives for over 25 years. He has received eleven IEEE prize paper awards for his work including co-recipient of the Best Paper Award in the IEEE Industry Applications Society Transactions for the year 1984. In 1986 he received the Outstanding Achievement Award from the IEEE Industry Applications Society for his contributions to the field of ac drives and in 1990 he received the William E. Newell Award of the IEEE Power Electronics Society for his contributions to power electronics.

J. Coleman White was Manager of the Rotating Machinery Program of the Electric Power Research Institute. He is presently retired. He was responsible for research and development concerned with turbine availability, controls and automation, motors and generators, and all other fossil plant electrical equipment. He earned the BEE degree from Cornell University in 1947, following service in the next 32 years with General Electric, responsible for the design and development of hydrogenerators, induction and synchronous motors and generators, and large direct current machines. Mr. White is a Fellow of the Institute of Electrical and Electronics Engineers, and the recipient of the 1987 Tesla Award. Active on many IEEE committees, he has also served as Chairman of the ANSI C50 Committee on Motors and Generators. He is a registered professional engineer in the State of New York.